

Separation of Coupling Coefficient Between Resonators into Magnetic and Electric Components Toward Its Application to BPF Development

Ikuo Awai, Yangjun Zhang

Department of Electronics & Informatics, Ryukoku University 1-5 Yokotani, Seta-oecho, Otsu 520-2194, Japan
Email: awai@rins.ryukoku.ac.jp, zhang@rins.ryukoku.ac.jp

Abstract A new concept on resonator's coupling coefficient is applied to various structures. The main idea is to discriminate the magnetic and electric contributions based on the coupled mode theory. Strong to weak coupling of open-ring resonators when they are faced on broadsides, is clarified together with the magnetic coupling's survival at the long distance. Combline and interdigital couplings are well explained to have different coupling property. Some new BPFs are proposed on the basis of the present theory, which could realize significant miniaturization of multi-stage BPFs.

Key words coupling coefficient, magnetic coupling, electric coupling, overlap integral

1. Introduction

Coupling coefficient of resonators is widely used for the filter design, but its physical meaning has seldom been discussed. The simple and powerful equation using the difference and sum of the split resonant frequencies has long been used for the coupling coefficient in the experiment as well as simulation without inquiry of the meaning.

$$k = \frac{2(\omega_h - \omega_l)}{\omega_h + \omega_l} \quad (1)$$

In the mean time, one of the present authors discussed its meaning and traced it as the energy exchange rate between two resonators [1], which was the explanation from the energy concept for the first time. The coupled mode theory used for the study above, gave rise to the side product, the overlap integral expression of the coupling coefficient.

It decomposes the coupling coefficient into the magnetic and electric components, which is quite useful for understanding and predicting the coupling of resonators. The present article will give clear insight into several interesting structures based on the decomposition theory.

2. Brief explanation of theory

According to the perturbation theory, the electromagnetic field of two coupled resonators is expressed with the linear combination of the eigen modes for the original uncoupled resonators.

$$\mathbf{E} = \sum_i^2 a_i \mathbf{E}_i \quad \mathbf{H} = \sum_i^2 b_i \mathbf{H}_i \quad (2)$$

Substituting the coupled field expression into Maxwell's equations, the differential equations for the field amplitude of each resonator are derived, which describe the energy exchange between two resonators.

$$\begin{aligned} \frac{d^2 a_1}{dt^2} + \omega_r^2 a_1 + \omega_r^2 k a_2 &= 0 \\ \frac{d^2 a_2}{dt^2} + \omega_r^2 a_2 + \omega_r^2 k a_1 &= 0 \end{aligned} \quad (3)$$

where ω_r is the resonant frequency of the uncoupled resonators.

The rate of energy exchange is given as subtraction of the overlap integrals of each resonator's electric and magnetic fields, and it is nothing but the coupling coefficient between two resonators [2].

$$k = \frac{\int_V \mu \mathbf{H}_1 \cdot \mathbf{H}_2^* dv - \int_V \epsilon \mathbf{E}_1 \cdot \mathbf{E}_2^* dv}{\int_V \epsilon |\mathbf{E}|^2 dv} \quad (4)$$

3. Role exchange of electric and magnetic couplings

3.1 Narrow-side coupled open ring resonators

Since an open ring resonator is essentially a half-wavelength resonator, the electric field is strong at the ends of the resonator, while the magnetic field is strong around its middle. Therefore, the configuration (a) in Fig. 1 couples rather electrically, while (c) magnetically [3]. The configuration (b) has weak coupling due to cancellation of magnetic and electric components. Typical examples are shown in Fig. 2 for these 3 different cases. They are in the microstrip configuration where the substrate thickness is 0.7mm, and permittivity $3.27\epsilon_0$.

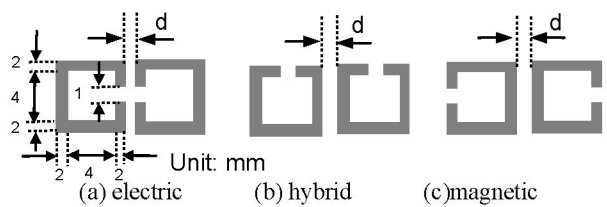


Fig. 1 Three typical coupling for open ring resonators

It is noted that (b) gives zero coupling at $d=1.0\text{mm}$ and magnetic coupling dominates for the larger distance. Magnetic coupling always survives in a distant place, because electric lines of force are terminated by the electric wall, whereas the magnetic wall does not exist to terminate the magnetic lines of force. Fig. 3 shows the coupling coefficient for the configuration (b) with the ground plane farther (The substrate thickness is increased into 1.4mm from 0.7mm). The electric coupling survives for the longer distance as expected.

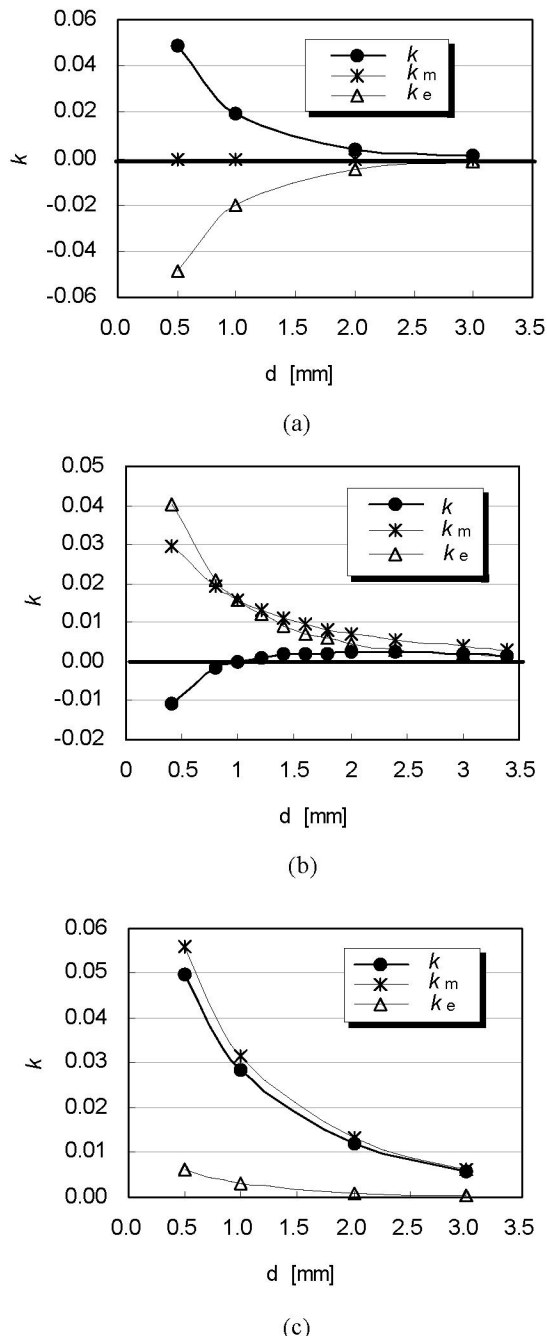


Fig. 2 Decomposition of coupling coefficient for (a), (b) and (c) cases in Fig.1

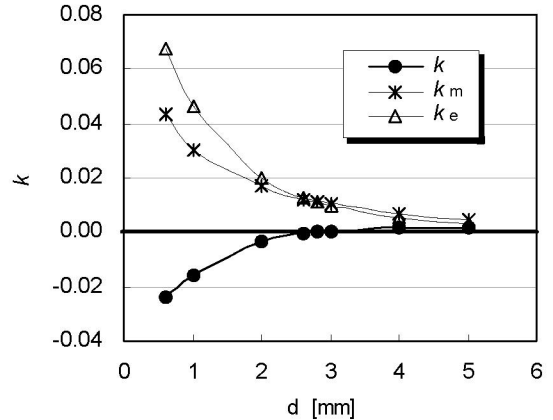


Fig. 3 Coupling coefficient for structure (b) in Fig.1 with farther ground plane

3.2 Broad-side coupled open ring resonators

In Fig. 4, a pair of open-ring resonators are shown to be coupled on the broad-side. There are two ground planes on the upper and lower sides of the resonators. They are 4mm apart from the resonators that are suspended in the free space. When one of the resonators rotates as shown in the Fig., the electric coupling changes quite much from positive to negative values and the total coupling coefficient ranges from 0.1 to 0.6, giving 6 times difference by rotation (Fig. 5). The qualitative explanation in Fig.6 will assist to understand the wide range variance of the coupling.

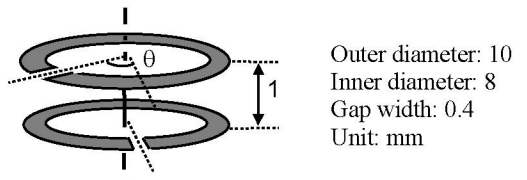


Fig. 4 Mutual rotation angle of broad-side coupled open ring resonators

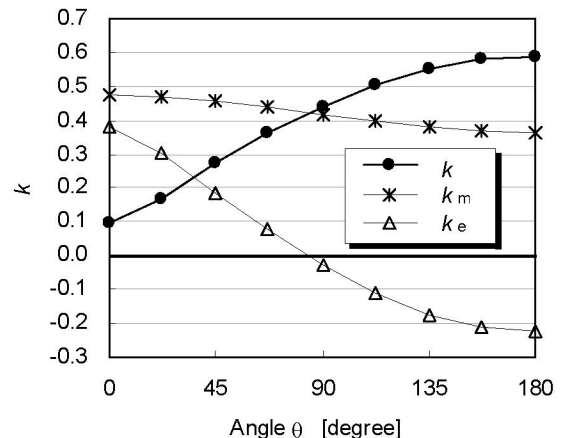


Fig. 5 Coupling coefficient of rotated open ring resonators

Each resonator is extended straight for easier comparison of the electromagnetic field distribution. Multiplication of magnetic fields for two resonators and its integration along the longitudinal direction is compared with that for the electric fields. In the case $\theta=0$, they are subtracted each other, but when $\theta=180$ degree, they are added, on the contrary, due to the opposite signs.

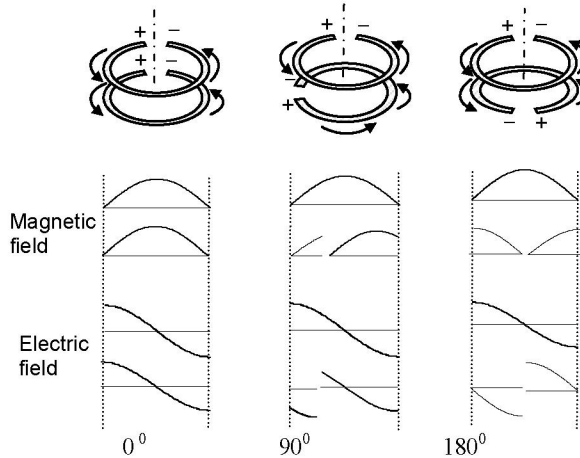


Fig. 6 Electromagnetic field distribution along open ring resonators

4. Comparison of narrow and broad-side couplings

Though the combline configuration is known to show rather weak coupling, broad-side coupled resonators may make it stronger. Fig. 7 shows the calculated results for both narrow and broad-side couplings, evidently indicating that larger coupling coefficient is obtained for the broadside coupling. Though the narrow-side coupled resonators are in the microstrip line configuration as Fig. 1, two ground planes exist at the upper and lower sides of resonators 4mm apart from the resonators that are suspended in the free space for the broad-side coupling.

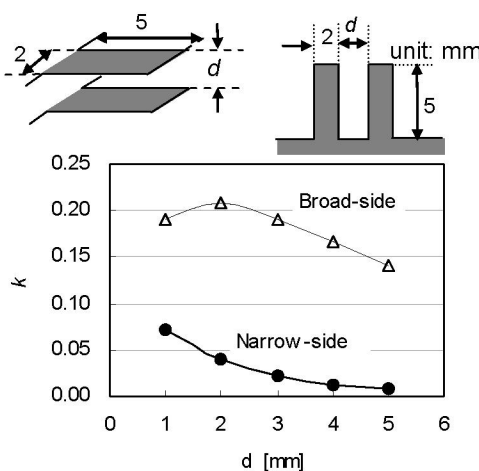


Fig. 7 Coupling coefficient for combline resonators with broad or narrow side coupling

The significant point for the broad-side coupling is that the coupling coefficient is almost constant irrespective of the resonator distance. It is because the magnetic and electric components of overlap integral are of the same sign to cancel each other. Each coupling coefficient is quite large (Fig. 8) because of the same patterns of E/M field distribution as shown in Fig. 9 in addition to the broadside coupling. The coupling naturally decreases as they separate each other. But the magnetic coupling decreases more slowly than the electric coupling as was explained before, and hence, the total coupling keeps the almost constant value.

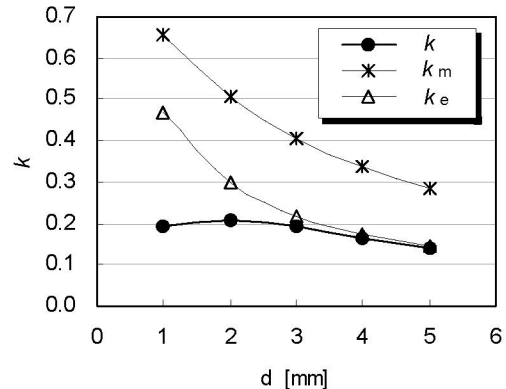


Fig. 8 Magnetic and electric components of coupling coefficient for broad-side coupled combline resonators

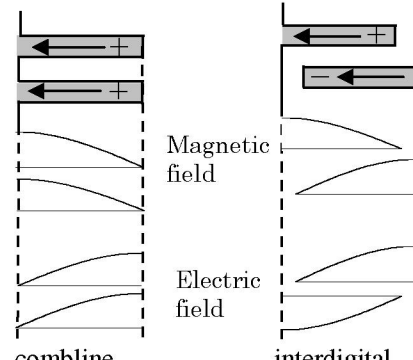


Fig. 9 Field distribution along $1/4$ resonators for combline and interdigital configuration

5. Comparison of interdigital and combline couplings

The interdigital configuration generally gives a stronger coupling coefficient than the combline configuration, since the magnetic and electric contribution add together as shown in Fig. 9. But each component has smaller values, since their field distributions do not coincide each other very well, giving smaller amplitude of overlap integral as is indicated in Fig. 9.

Fig. 10 shows the comparison of narrow-side coupled interdigital and combline configurations with ground planes added at the lower side from the resonators making a microstrip line structure in the same way as Fig.

1. Dependence on the resonator distance for the interdigital configuration is stronger than the combline counterpart, rapid increase being observed for shorter distances.

6. Application to BPF development

We have studied that magnetic and electric couplings add or subtract each other to result strong or weak coupling, respectively, depending on the configuration. Strong coupling is used for a broad band BPF, while weak coupling is for a narrow band BPF.

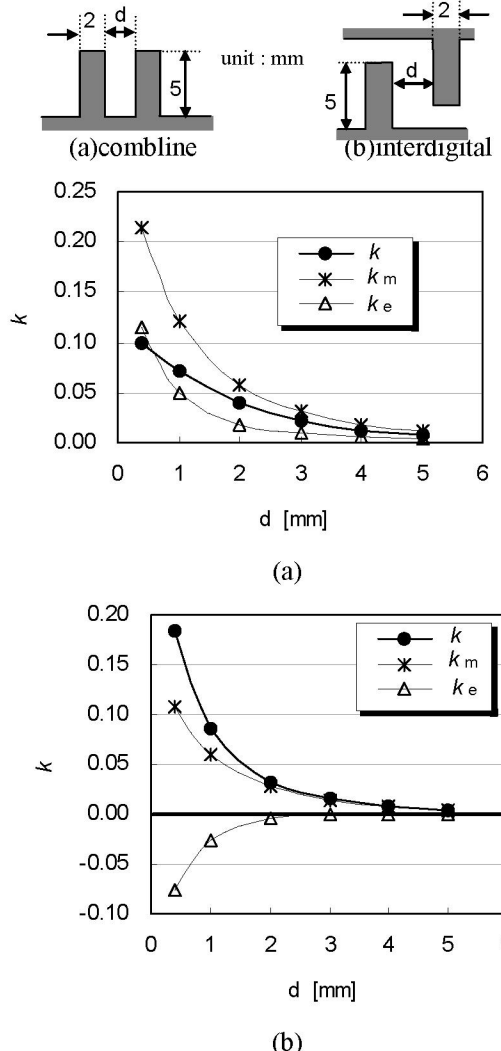


Fig. 10 Magnetic and electric components of coupling coefficient for narrow-side coupled combline and interdigital resonators

Strong coupling is usually realized by broad-side coupling as was shown in Fig. 7. But weak coupling is somehow attained by broadside coupling due to subtraction of magnetic and electric components.

The advantage of broad-side coupled resonators is to fabricate a low profile BPF with a constant foot print. But if one uses more than 2 resonators in the stripline

configuration, intermediate resonators do not have the ground plane close to them as shown in Fig. 11, and thus, the coupling coefficient or other parameters are not defined well.

Therefore, we will use the coplanar structure having the connected ground plane for each resonator. The ground planes are also effective to suppress the jump coupling over adjacent resonators.

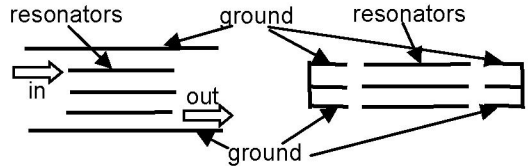


Fig. 11 Comparison of ground planes for broadside coupled stripline and coplanar BPFs

6.1 Open ring resonator BPF

The metal pattern of the proposed BPF is depicted in Fig. 12 as a 2-stage version. These are sandwiched between substrates with permittivity $3.27\epsilon_0$. Multi-stage BPF would be easily fabricated piling up the substrates. The thickness of substrate is made as thin as possible, which helps to make it of low profile and give another new property: the variable range of coupling coefficient is extended. Fig. 13 is the calculated result for the distance $d=0.2\text{mm}$, which indicates the coupling coefficient is controllable from 0.04 to 0.8 by rotating the resonator in the same way as Fig. 4. It should be noted that the controllable range is increased into 20 times compared with 6 times for the case in Fig. 5.

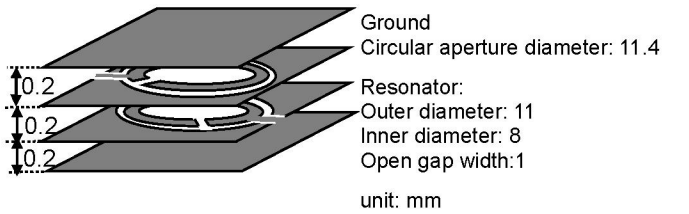


Fig. 12 Proposed open ring resonator BPF

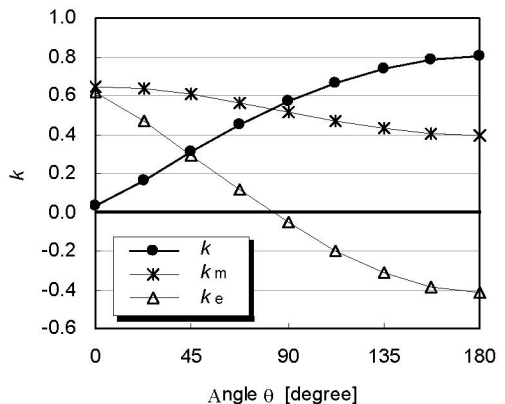


Fig. 13 Coupling coefficient for coplanar open ring resonators.

The external Q is also controlled by rotation of the external transmission lines, which is shown in Fig. 14. This data is used for matching the circuit.

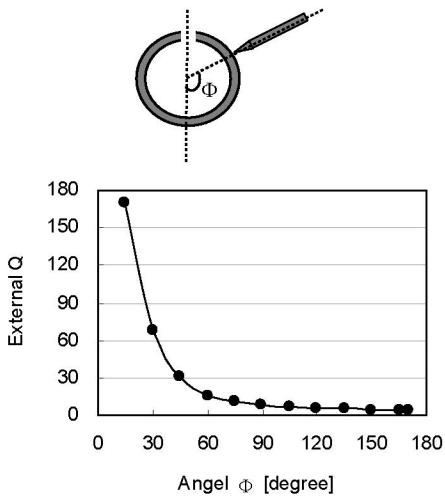


Fig. 14 External Q versus excitation angle for broad-side coupled coplanar open ring resonator

6.2 Comline and interdigital BPF

Comline coupling also becomes very small by decreasing the distance between resonators, because the magnetic and electric components become of the same amplitude due to the decrease of fringing field and cancel each other perfectly. Fig. 15 shows the variation of coupling as a function of the metal shield. Two ground planes are assumed in the same way as Fig. 12

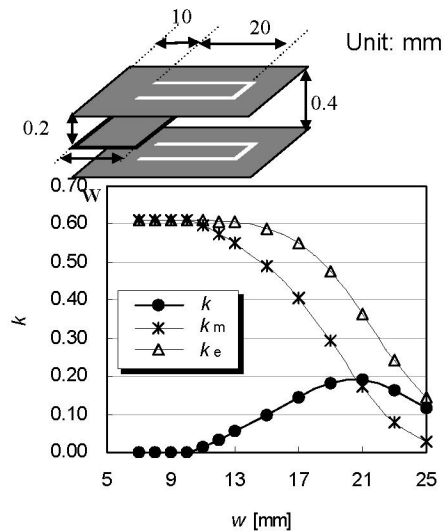


Fig. 15 Coupling coefficient for broad-side coupled coplanar comline resonators

The unique point for this structure is that the coupling increases as one inserts a shield plate between the resonators, to the contrary for a common resonator coupling. It is simply because the balance is destroyed to

induce the remnant coupling. The coefficient from 0 to 0.2 is realizable by the comline structure.

Larger coupling is obtained by the interdigital structure. The maximum coupling coefficient 0.8 is reduced by the inserted metal shield as shown in Fig. 16. The variable range is so wide that it can cope with the demand for narrow to wide band BPFs.

These two structures are also applicable to the low profile, small footprint BPF, and hence, we will design and fabricate them in the near future.

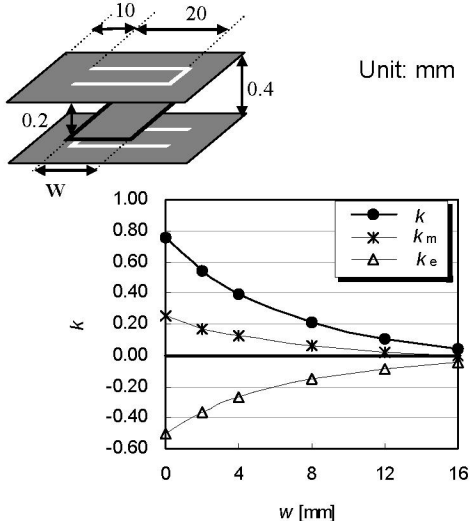


Fig. 16 Coupling coefficient for broad-side coupled coplanar interdigital resonators

7. Conclusion

Coupling coefficient of resonators is decomposed into the magnetic and electric contributions based on the coupled mode theory. The following typical structures have been addressed and compared.

- (1) Narrow -side coupled open ring resonators
- (2) Broad-side coupled open ring resonators
- (3) Comline resonators
- (4) Interdigital resonators
- (5) Proposal of broadside coupled resonator BPFs

References

- [1] I. Awai, "New Expressions for Coupling Coefficient between Resonators", IEICE Trans. Electron., E88C, No.12, Dec. 2005
- [2] Ikuo Awai and Yangjun Zhang, "Overlap integral calculation of resonator coupling", Proceedings of 12th International Symposium on Antenna Technology and Applied Electromagnetics and URSI/CNC Conference, pp. 589-592, Montreal, July 2006.
- [3] J. S. Hong and M. J. Lancaster, Microstrip filters for rf/microwave applications, John Wiley & Sons Inc., New York, 2001